



Universiteit  
Leiden  
The Netherlands

## Neuroimaging findings in retinal vasculopathy with cerebral leukoencephalopathy and systemic manifestations

Hoogeveen, E.S.; Pelzer, N.; Boer, I. de; Buchem, M.A. van; Terwindt, G.M.; Kruit, M.C.



### Citation

Hoogeveen, E. S., Pelzer, N., Boer, I. de, Buchem, M. A. van, Terwindt, G. M., & Kruit, M. C. (2021). Neuroimaging findings in retinal vasculopathy with cerebral leukoencephalopathy and systemic manifestations. *American Journal Of Neuroradiology*, 42(9), 1604-1609. doi:10.3174/ajnr.A7194

Version: Not Applicable (or Unknown)  
License: [Leiden University Non-exclusive license](#)  
Downloaded from: <https://hdl.handle.net/1887/3248732>

**Note:** To cite this publication please use the final published version (if applicable).

# Neuroimaging Findings in Retinal Vasculopathy with Cerebral Leukoencephalopathy and Systemic Manifestations

 E.S. Hoogeveen,  N. Pelzer,  I. de Boer,  M.A. van Buchem,  G.M. Terwindt, and  M.C. Kruit



## ABSTRACT

**SUMMARY:** Retinal vasculopathy with cerebral leukoencephalopathy and systemic manifestations is caused by *TREX1* mutations. High-quality systematic follow-up neuroimaging findings have not been described in presymptomatic and symptomatic mutation carriers. We present MR imaging findings of 29 *TREX1* mutation carriers (20–65 years of age) and follow-up of 17 mutation carriers (30–65 years of age). Mutation carriers younger than 40 years of age showed a notable number of punctate white matter lesions, but scan findings were generally unremarkable. From 40 years of age onward, supratentorial lesions developed with long-term contrast enhancement (median, 24 months) and diffusion restriction (median, 8 months). In these lesions, central susceptibility artifacts developed, at least partly corresponding to calcifications on available CT scans. Some lesions ( $n=2$ ) additionally showed surrounding edema and mass effect (pseudotumors). Cerebellar punctate enhancing lesions developed mainly in individuals older than 50 years of age. These typical neuroimaging findings should aid neuroradiologic recognition of retinal vasculopathy with cerebral leukoencephalopathy and systemic manifestations, which may enable early treatment of manifestations of the disease.

**ABBREVIATIONS:** Gd = gadolinium; MC = mutation carrier; RVCL-S = retinal vasculopathy with cerebral leukoencephalopathy and systemic manifestations; WML = white matter lesion

Retinal vasculopathy with cerebral leukoencephalopathy and systemic manifestations (RVCL-S) is a dominantly inherited disease caused by mutations in the *TREX1* gene.<sup>1</sup> RVCL-S is histologically characterized by a systemic vasculopathy of medium- and small-caliber arteries as well as veins.<sup>2,3</sup> Clinically, the disease manifests from 35 to 40 years of age onward and is characterized by vascular retinopathy, Raynaud phenomenon, migraine, and dysfunction of multiple internal organs (including kidney disease, liver disease, anemia, and subclinical hypothyroidism).<sup>4</sup>

So far, few studies have described neuroimaging findings, mostly in symptomatic RVCL-S patients with advanced disease.<sup>2,5-17</sup> A previous study described 3 types of lesions: 1) focal-to-confluent

nonenhancing white matter lesions (WMLs), 2) WMLs with punctate enhancement, and 3) rim-enhancing lesions with surrounding T2-hyperintensity (edema/gliosis) and/or diffusion restriction.<sup>9</sup> These lesions with surrounding edema may become large with mass effect and are referred to as pseudotumors.

RVCL-S remains a frequently missed diagnosis, partly due to lack of recognition by radiologists. We systematically studied the neuroimaging characteristics of RVCL-S and describe the frequency and evolution of these findings in a large set of presymptomatic and symptomatic carriers.

## MATERIALS AND METHODS

### Participants

All family members 18 years of age and older from 3 unrelated Dutch families with RVCL-S were invited to participate in this study. Family members with unknown *TREX1* status were genetically tested. The genetic status of individuals was not disclosed to them, unless specifically requested. The study was approved by the local Medical Ethics Committee. All participants provided written informed consent before inclusion. The study was performed according to guidelines of the Declaration of Helsinki.

### Study Design

The study design has been described in a previous publication in which baseline clinical data of the mutation carriers (MCs) was

Received January 18, 2021; accepted after revision April 12.


From the Departments of Radiology (E.S.H., M.A.v.B., M.C.K.) and Neurology (N.P., I.d.B., G.M.T.), Leiden University Medical Center, Leiden, the Netherlands.

G.M. Terwindt and M.C. Kruit shared last authorship.

This study was supported by the Dutch Organization for Scientific Research (GT: VIDI 917-11-31), Stichting Dioraphte (GT: 20010407), and the International Retinal Research Foundation (GT, IdB: IRR-RVCL-S 2019).

The funders had no role in the design or conduct of the study.

Please address correspondence to Mark C. Kruit, MD, PhD, Leiden University Medical Center, Department of Radiology, P.O. Box 9600, 2300 RC Leiden, the Netherlands; e-mail: m.c.kruit@lumc.nl

 Indicates open access to non-subscribers at [www.ajnr.org](http://www.ajnr.org)

 Indicates article with online supplemental data.

<http://dx.doi.org/10.3174/ajnr.A7194>

**Table 1: MR imaging markers in *TREX1* MCs at baseline<sup>a</sup>**

| MR Imaging Markers           | All (n = 29)   | Younger than 40 Years (n = 11) | 40 Years or Older (n = 18) |
|------------------------------|----------------|--------------------------------|----------------------------|
| WMLs (mL), median (IQR)      | 0.97 (0.2–3.9) | 0.19 (0.08–0.3)                | 2.66 (1.0–7.7)             |
| Deep WMLs                    |                |                                |                            |
| Absent                       | 8 (28)         | 6 (55)                         | 2 (11)                     |
| Punctate lesions             | 18 (62)        | 5 (45)                         | 13 (72)                    |
| Beginning confluence         | 2 (7)          | 0                              | 2 (11)                     |
| Large confluent areas        | 1 (3)          | 0                              | 1 (6)                      |
| Periventricular WMLs         |                |                                |                            |
| Absent                       | 19 (66)        | 9 (82)                         | 10 (55)                    |
| Caps and bands               | 2 (7)          | 2 (18)                         | 0                          |
| Smooth halo                  | 5 (17)         | 0                              | 5 (28)                     |
| Irregular extending in DWM   | 3 (10)         | 0                              | 3 (17)                     |
| Enlarged perivascular spaces |                |                                |                            |
| None                         | 12 (41)        | 4 (36)                         | 8 (44)                     |
| Mild                         | 14 (48)        | 6 (55)                         | 8 (44)                     |
| Moderate                     | 2 (7)          | 0                              | 2 (11)                     |
| Frequent                     | 1 (3)          | 1 (9)                          | 0                          |
| Central atrophy              |                |                                |                            |
| None                         | 24 (83)        | 11 (100)                       | 13 (72)                    |
| Moderate                     | 5 (17)         | 0                              | 5 (28)                     |
| Severe                       | 0              | 0                              | 0                          |
| Cortical atrophy             |                |                                |                            |
| None                         | 27 (93)        | 11 (100)                       | 16 (89)                    |
| Moderate                     | 2 (7)          | 0                              | 2 (11)                     |
| Severe                       | 0              | 0                              | 0                          |
| Lacunar infarcts             | 1 (3)          | 0                              | 1 (6)                      |

**Note:**—IQR indicates interquartile range; DWM, deep white matter.

<sup>a</sup>Data are No. (%) unless otherwise specified.

presented.<sup>4</sup> In short, all MCs underwent a baseline MR imaging for research purposes only. Follow-up imaging was acquired only in *TREX1* MCs who were aware of their genetic status for combined clinical and research purposes, using the same MR imaging scanner and scan protocol. In addition, CT scans acquired for clinical purposes during the follow-up period were included in the evaluation. The 3T MR imaging scanning protocol consisted of pre- and postgadolinium 3D-T1-weighted, 3D-FLAIR, DWI, SWI, and T2-weighted scans (Online Supplemental Data).

### Measurements

The age of MCs was rounded to the nearest half-decade to protect anonymity.

General features of small-vessel disease were evaluated on baseline scans using predefined criteria (Online Supplemental Data).

As earlier described, active RVCL-S lesions were those with punctiform, linear, or rim gadolinium (Gd) enhancement and/or diffusion restriction.<sup>9</sup> Number, location, and, if available, behavior across time were recorded. Colocalization of susceptibility artifacts on SWI was recorded. At follow-up, the duration of enhancement and diffusion restriction of lesions was assessed, defined as visible on at least 2 consecutive time points.

### RESULTS

Baseline MR images were available in 29 MCs (17 women) with a median age of 51 years (range, 20–65 years). Follow-up MR images were available in 17 MCs (12 women) with a median age of 53 years (range, 30–65 years). The median follow-up time between baseline and the last MR imaging was 29 months (range, 20–36 months) with a median of 2 follow-up scans per MC (range, 1–7 MR images). For 2 MCs, additional CT scans were available.

### Cross-Sectional Neuroimaging Characteristics

Baseline characteristics of small-vessel disease are presented in Table 1. Already, 45% of the MCs younger than

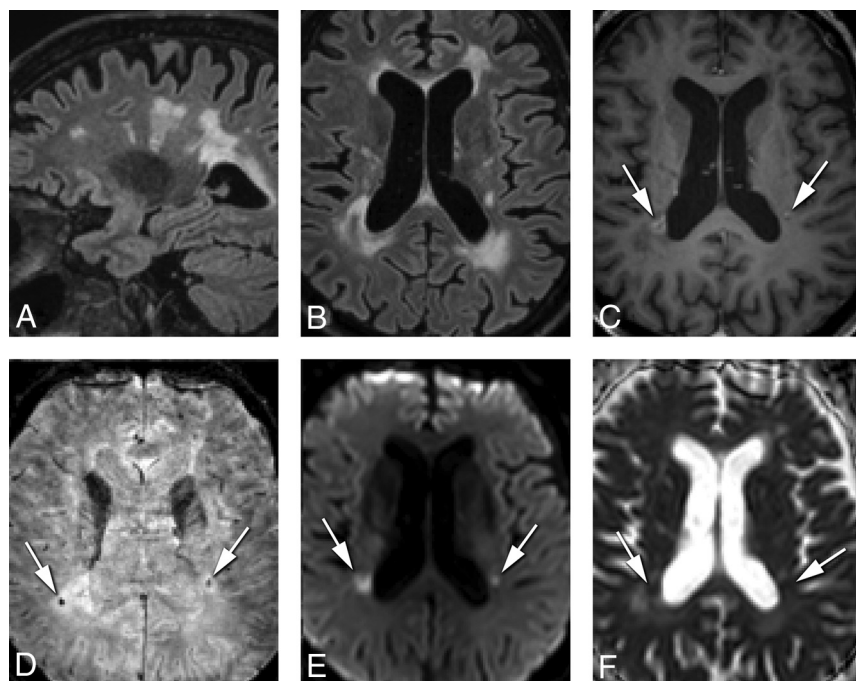


**FIG 1.** MR imaging characteristics of typical RVCL-S lesions in a 60-year-old man. Periventricular and deep WMLs on sagittal (A) and transverse FLAIR (B) images. On the 3D-T1-weighted Gd image (C), note a rim-enhancing lesion next to the right dorsal horn and a punctiform enhancing lesion next to the left dorsal horn (white arrows). Punctiform SWI artifacts are seen in the center of these lesions (D). High DWI (E) and low ADC signal (F) in the lesions correspond to diffusion restriction.

40 years of age showed punctate WMLs, more than expected for their age. In MCs 40 years of age or older, various degrees of white matter involvement were documented and most WMLs were located in the supratentorial periventricular and deep white matter. In contrast to earlier reports,<sup>3,9</sup> the corpus callosum was also affected in a few cases with extensive WMLs. In 1 case, WMLs even seemed to have a characteristic Dawson fingers pattern (Fig 1). This MC did not have a clinical diagnosis of multiple sclerosis; however, a radiologically isolated syndrome of multiple sclerosis was not fully excluded because no CSF analyses or spinal MR images were obtained.

In total, 10 MCs showed  $\geq 1$  supratentorial active lesion at baseline; the youngest was 40 years of age. In these 10 MCs, a total of 44 active supratentorial RVCL-S lesions were identified. Their neuroimaging characteristics are presented in Table 2. All basal ganglia lesions showed punctiform enhancement (Fig 2). Linear or rim-enhancing lesions were mostly next to the frontal ( $n = 6$ ) or dorsal horns ( $n = 5$ ) of the lateral ventricles. Diffusion restriction was observed mainly in the center of lesions, except in a few larger

lesions ( $n = 2$ ) in which restriction was at the periphery. Central punctiform or linear susceptibility artifacts were noted in 68% of lesions (Fig 1). All rim-enhancing lesions showed diffusion restriction and susceptibility artifacts. Although 1 rim-enhancing lesion had some associated edema, no pseudotumors were present at baseline. At baseline, 20 MCs were aware of their mutation status and were tested for vascular retinopathy. Nineteen MCs had signs of retinopathy (mean age, 53 [SD, 8] years). Of these, 10 (53%) had  $\geq 1$  supratentorial active lesion. The MC without retinopathy (50 years of age) did not have active lesions. Due to ethical concerns, MCs who did not wish to know their mutation status could not be tested for retinopathy ( $n = 9$ ; mean age, 26 [SD, 5] years). None of them had active lesions. At baseline, 11/29 MCs (38%) had features of focal or global brain dysfunction, and 6/29 MCs (21%) had internal organ dysfunction (Online Supplemental Data).

Eight MCs (all older than 50 years of age) had cerebellar punctiform enhancing lesions at baseline (range, 1–16; 75% bilaterally; Fig 2). Eight lesions (20%) had central susceptibility artifacts; none showed diffusion restriction.

**Table 2: Characteristics of active RVCL-S lesions at baseline**

|                               | All Lesions (N = 44) No. (%) |
|-------------------------------|------------------------------|
| Size in mm, median (IQR)      | 4 (2–8)                      |
| Location                      |                              |
| Periventricular               | 12 (27)                      |
| Deep/subcortical white matter | 17 (39)                      |
| Basal ganglia/thalamus        | 15 (34)                      |
| Characteristics of activity   |                              |
| Enhancement                   |                              |
| Unknown <sup>a</sup>          | 2 (4)                        |
| No enhancement                | 2 (4)                        |
| Punctiform enhancement        | 24 (55)                      |
| Linear enhancement            | 6 (14)                       |
| Rim enhancement               | 10 (23)                      |
| Diffusion restriction         | 22 (50)                      |
| Other characteristics         |                              |
| T2-hyperintensity             | 33 (75)                      |
| Susceptibility artifacts      | 30 (68)                      |
| Mass effect                   | 0                            |

<sup>a</sup>In 1 MC, no contrast was administered due to reduced kidney function. Lesions in this MC showed diffusion restriction.

### Follow-up Neuroimaging Characteristics

In 5 MCs (4 women; median age, 52 years; range, 30–60 years), no active supratentorial lesions were observed at all, and 1 MC did not develop new lesions during follow-up. Of these, 4/6 MCs had signs of vascular retinopathy. In 11/17 (65%) MCs, a total of 28 new supratentorial lesions developed (Online Supplemental Data). All 11 MCs had signs of vascular retinopathy. During follow-up, 11/17 MCs (65%) had features of focal or global brain dysfunction and 8/17 MCs (47%) had internal organ dysfunction (Online Supplemental Data). We observed long-term enhancement in 46/72 (64%) lesions and long-term diffusion restriction in 26/72 (36%) lesions. In these lesions, contrast enhancement persisted for a median of 24 months (range, 2–37 months), and diffusion restriction, for 8 months (range, 3–32 months). Figure 3 illustrates long-term enhancement and diffusion restriction during 31 months of follow-up. Most lesions appeared at a certain time point, remained unchanged for a period of time, and eventually became smaller and disappeared with or without a residual lesion of gliosis and/or SWI artifacts. Six lesions were visually documented to increase in size.

Almost exclusively, lesions located in the deep and periventricular white matter became linear or rim-enhancing lesions, while the enhancement of lesions in the basal ganglia remained punctiform. Two MCs (12%) developed a rim-enhancing mass lesion with surrounding edema (pseudotumor) during follow-up (Figs 4 and 5). Both MCs received corticosteroid treatment after the first evidence of the pseudotumor, after which the pseudotumor gradually diminished in size (Fig 5). In 1 of these MCs, we noted, on consecutively acquired CT scans, the development of a punctiform calcification corresponding to SWI artifacts as long as 31 months after the first evidence of the

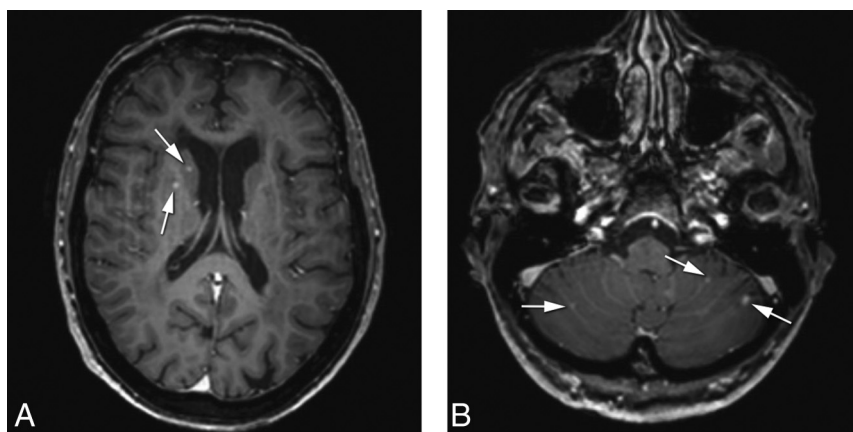


**FIG 2.** An example of punctiform enhancing lesions in the basal ganglia and cerebellum in a 60-year-old woman. *A*, Punctiform enhancing lesions (white arrows) in the putamen and caudate head on the right. *B*, Bilateral punctiform enhancing cerebellar lesions (white arrows).

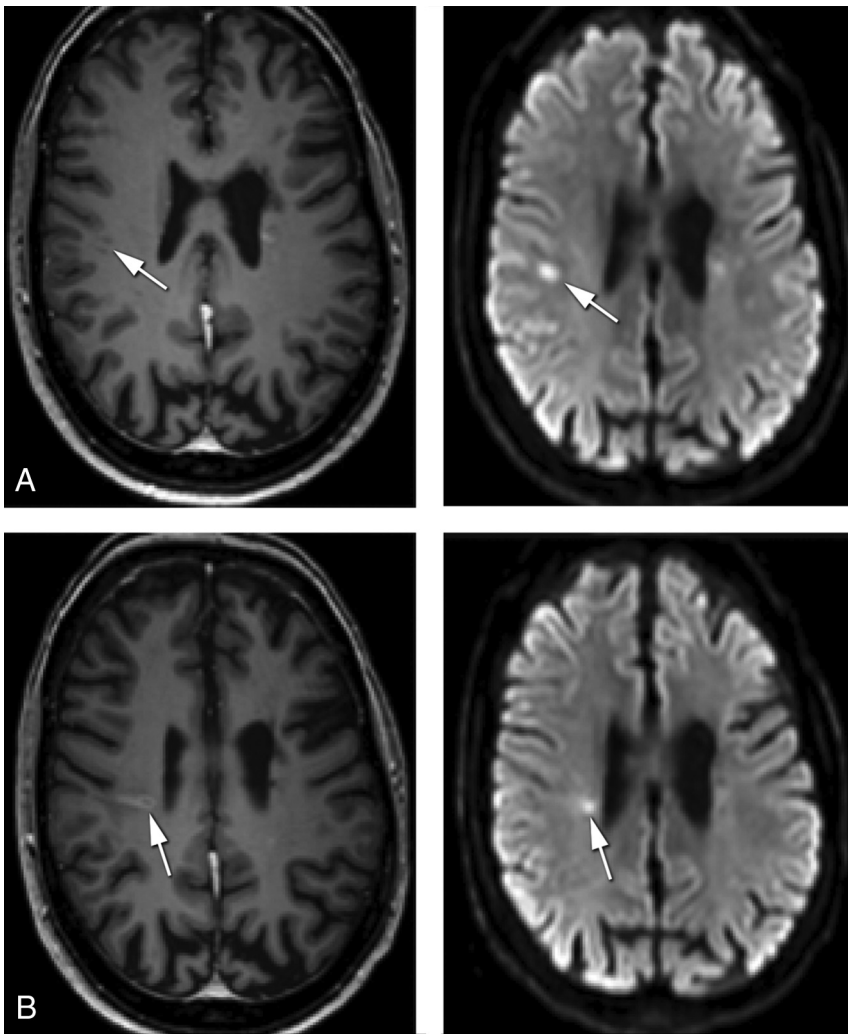


**FIG 3.** Long-term enhancement and diffusion restriction of a lesion during 31 months of follow-up in a 55-year-old woman. 3D-T1-weighted Gd and diffusion-weighted images acquired at baseline (A) show a punctiform enhancing lesion on the right with subtle diffusion restriction (*white arrows*), and after 31 months (B), the images show that the lesion migrates to the right ventricle (*white arrows*). The lesion is now linearly enhancing with partial rim enhancement and diffusion restriction (ADC with low values is not shown).

pseudotumor (Fig 5 and Online Supplemental Data). In 1 other MC, additional CT images were available in which multiple punctiform calcifications corresponded with part of the susceptibility artifacts on the SWI (data not shown).

Five MCs showed an increase in the number of enhancing punctiform cerebellar lesions. Two MCs developed a small rim-enhancing cerebellar lesion with associated T2 and FLAIR hyperintensity; of these, 1 also showed susceptibility artifacts. None of the cerebellar lesions showed diffusion restriction.

## DISCUSSION

This study systematically reports neuroimaging findings in a group of MCs with RVCL-S in a broad age range, enabling us to describe the presentation and natural history of both subtle and more obvious MR imaging features of the disease. Recognition of these

imaging features and the evolution of lesions with time may help to diagnose RVCL-S earlier.

In MCs younger than 40 years, who were mostly clinically asymptomatic, 45% had nonspecific supratentorial punctiform WMLs, remarkable for this age. One recent study also reported WMLs in 5 patients with RVCL-S younger than 40 years of age with comparable WML volumes.<sup>17</sup> Nonspecific WMLs become more apparent in individuals older than 40 years of age. While some MCs still have only discrete punctate WMLs, some develop more extensive confluent WMLs.

Starting from 40 years of age, supratentorial “active” lesions (with contrast enhancement and/or diffusion restriction) may develop and become more prevalent with increasing age. These active lesions were present in 50% of MCs in the 40 years and older age group. Most lesions were relatively small ( $\pm 4$  mm) and were equally distributed in the periventricular white matter, deep white matter, and basal ganglia, with rim-enhancing lesions mainly found in the deep and periventricular white matter. Before, only punctiform and rim-enhancing lesions were described as characteristic of RVCL-S,<sup>9</sup> however linear enhancing lesions can also be observed.

Follow-up MR imaging demonstrated that many active lesions remain stable or decrease in size and may show long-term persistence of enhancement and diffusion restriction. A general pattern is that RVCL-S lesions first show contrast enhancement as well as diffu-

sion restriction, and while the diffusion restriction fades away after a few months, the contrast enhancement can persist for up to 2 years. This is in accordance with a recent report in 6 symptomatic patients with RVCL-S, in which lesions showed a mean duration of diffusion restriction of 5 months and contrast enhancement of 20 months.<sup>16</sup> Why RVCL-S lesions show such long-term enhancement and diffusion restriction is not fully understood. Histopathologic findings in RVCL-S lesions show focal areas of tissue inflammation and necrosis, which resemble findings in delayed radiation necrosis. In RVCL-S, this is assumed to result from endothelial dysfunction with blood-brain barrier dysfunction and chronic ischemia.<sup>9</sup> The chronic nature of these focal areas of tissue inflammation and necrosis in RVCL-S may explain the long-term enhancement and diffusion restriction. Few lesions grew during follow-up, and in some lesions, a slow “migration” was observed, leaving earlier affected tissue behind as parenchymal loss/gliosis (Fig 3). In 2 cases, a pseudotumor

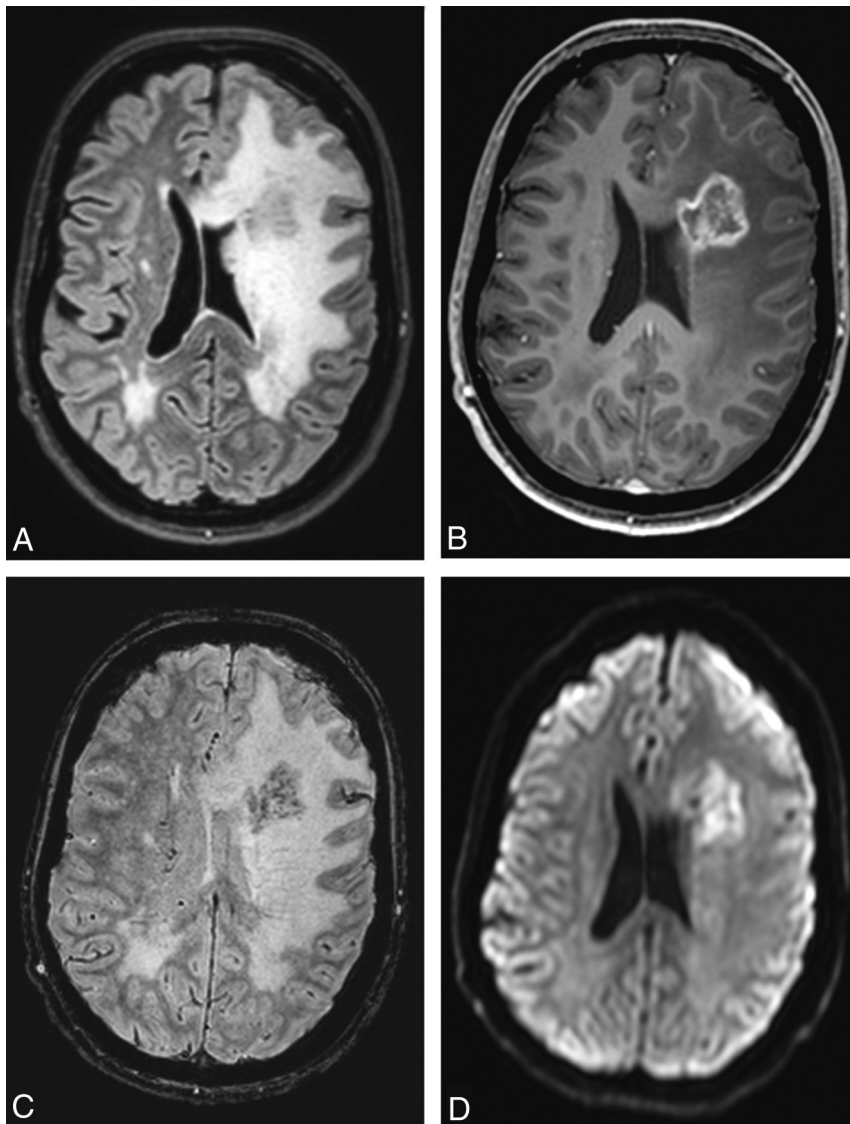


**FIG 4.** Imaging characteristics of a pseudotumor in a 45-year-old woman. Note a rim-enhancing lesion of 30 mm, craniolateral to the left frontal horn, with multiple dotlike susceptibility artifacts and diffusion restriction in the center of the lesion with extensive surrounding vasogenic edema with mass effect (A, FLAIR. B, 3DT1 Gd. C, SWI. D, DWI).

developed, which is much less frequent than previously reported.<sup>9</sup> This difference might be related to the younger age and fewer symptomatic cases in our study compared with previous literature.

RVCL-S was associated with multiple, bilateral, mostly punctiform enhancing cerebellar lesions, some with central susceptibility artifacts. Infratentorial lesions were also reported in a previous study.<sup>16</sup> A novel finding in this study is that these lesions start to develop with more advanced disease, around 50 years of age. Cerebellar lesions tend to progress in number, not so much in size. Only a few solitary cerebellar lesions grew in size with rim enhancement.

Up to 68% of active RVCL-S lesions were associated with susceptibility artifacts on the SWI scan, which may relate to extravasated blood products (hemosiderin), calcifications, or prominent vascular (venous) structures. Previously, RVCL-S was shown to

be associated with parenchymal calcification.<sup>9,15</sup> In Fig 5, we show that focal calcifications may develop some time after the formation of an active RVCL-S lesion, in this case, as long as 31 months after the first evidence of the RVCL-S lesion. Calcifications may occur as dystrophic changes in an area of chronic parenchyma damage or as a result of vessel injury. This possibility was shown in a recent histopathologic study, in which focal calcifications associated with WMLs and granular calcifications in the walls of several vessels were described.<sup>18</sup> In the current study, punctiform SWI artifacts were also seen in the basal ganglia and cerebellum. Proof of calcifications in the basal ganglia and cerebellar hemispheres would be a new finding in RVCL-S.<sup>9</sup>

In the past, neuroimaging findings of RVCL-S have been mistaken for multiple sclerosis, vasculitis, or neoplasms, and unnecessary brain biopsies have been performed in some cases.<sup>7,11</sup> Diffusion restriction may be falsely interpreted as a sign of ischemia or infarction, and the features of disrupted blood-brain barrier somewhat resemble late radiotherapeutic effects and necrosis. However, the long-lasting contrast enhancement and diffusion restriction of RVCL-S lesions have not been reported in any other brain disease.

## CONCLUSIONS

Although some neuroimaging characteristics in RVCL-S may be observed in other small-vessel diseases as well, the pattern and evolution of neuroimaging findings are typical for RVCL-S.

Mainly the long-term contrast enhancement with accompanying long-term diffusion restriction of RVCL-S lesions characterizes the disease. These findings, together with clinical features, should alert radiologists to consider the diagnosis of RVCL-S and enable early treatment of manifestations of the disease.

Disclosures: Irene de Boer—RELATED: Grant: Stichting Dioraphte and International Retinal Research Foundation\*; UNRELATED: Royalties: UpToDate. Gisela M. Terwindt—RELATED: Grant: Stichting Dioraphte and International Retinal Research Foundation\*; UNRELATED: Royalties: UpToDate. \*Money paid to the institution.

## REFERENCES

1. Richards A, van den Maagdenberg AM, Jen JC, et al. **C-terminal truncations in human 3'-5' DNA exonuclease TREX1 cause autosomal dominant retinal vasculopathy with cerebral leukodystrophy.** *Nat Genet* 2007;39:1068–70 [CrossRef Medline](#)

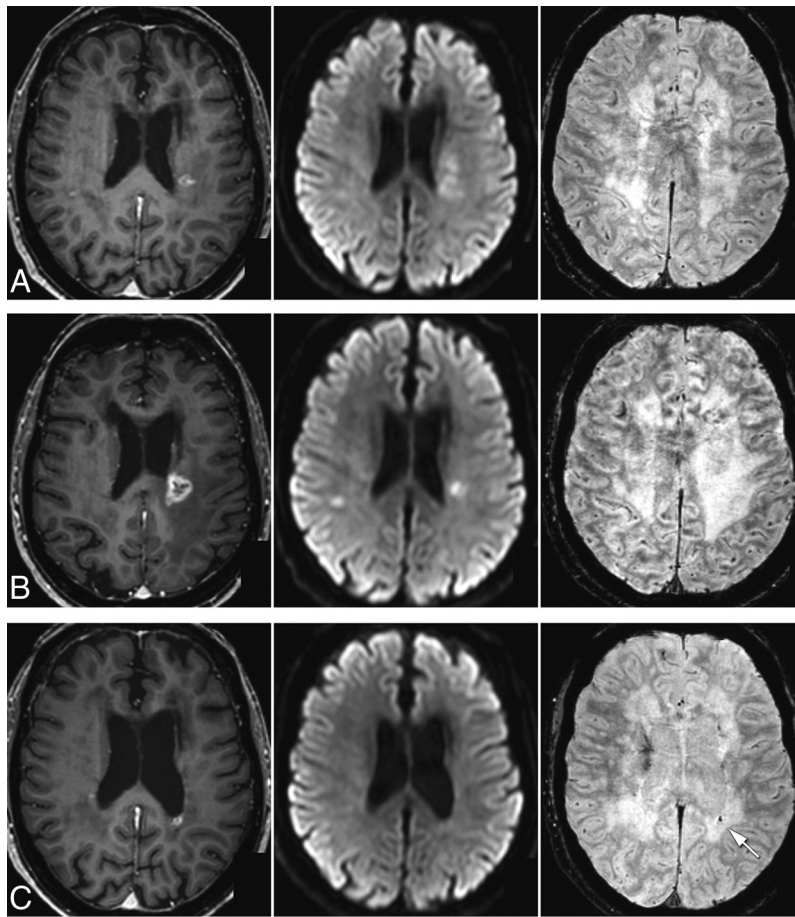


**FIG 5.** Imaging characteristics and evolution of a pseudotumor in a 60-year-old woman. 3D-T1-weighted Gd, diffusion-weighted, and SWI at baseline (A) show a rim-enhancing lesion with subtle diffusion restriction next to the left dorsal horn with some surrounding edema without mass effect. There were no abnormalities on the SWI. After 10 months (B), the lesion grows with new compression due to edema. Diffusion restriction is still noted, but no SWI abnormalities. After corticosteroid treatment, the enhancing lesion slowly diminished in size, and diffusion restriction disappeared at 31 months (C). A new SWI artefact in the center of the lesion is now noted (white arrow), corresponding to a focal calcification on CT acquired at 32 months, while at 15 months, no calcifications were present (Online Supplemental Data).

2. Jen J, Cohen AH, Yue Q, et al. **Hereditary endotheliopathy with retinopathy, nephropathy, and stroke (HERNS).** *Neurology* 1997;49:1322–30 [CrossRef Medline](#)
3. Kolar GR, Kothari PH, Khanlou N, et al. **Neuropathology and genetics of cerebroretinal vasculopathies.** *Brain Pathol* 2014;24:510–18 [CrossRef Medline](#)
4. Pelzer N, Hoogeveen ES, Haan J, et al. **Systemic features of retinal vasculopathy with cerebral leukoencephalopathy and systemic manifestations: a monogenic small vessel disease.** *J Intern Med* 2019;285:317–13 [CrossRef Medline](#)
5. Dhamija R, Schiff D, Lopes MB, et al. **Evolution of brain lesions in a patient with TREX1 cerebroretinal vasculopathy.** *Neurology* 2015;85:1633–34 [CrossRef Medline](#)
6. Terwindt GM, Haan J, Ophoff RA, et al. **Clinical and genetic analysis of a large Dutch family with autosomal dominant vascular**

**retinopathy, migraine and Raynaud's phenomenon.** *Brain* 1998;121:303–16 [CrossRef Medline](#)

7. Weil S, Reifemberger G, Dudel C, et al. **Cerebroretinal vasculopathy mimicking a brain tumor: a case of a rare hereditary syndrome.** *Neurology* 1999;53:629–31 [CrossRef Medline](#)
8. Mateen FJ, Krecke K, Younge BR, et al. **Evolution of a tumor-like lesion in cerebroretinal vasculopathy and TREX1 mutation.** *Neurology* 2010;75:1211–13 [CrossRef Medline](#)
9. Stam AH, Kothari PH, Shaikh A, et al. **Retinal vasculopathy with cerebral leukoencephalopathy and systemic manifestations.** *Brain* 2016;139:2909–22 [CrossRef Medline](#)
10. Monroy-Jaramillo N, Ceron A, Leon E, et al. **Phenotypic variability in a Mexican Mestizo family with retinal vasculopathy with cerebral leukodystrophy and TREX1 mutation p.V235Gfs\*6.** *Rev Invest Clin* 2018;70:68–75 [CrossRef Medline](#)
11. Hardy TA, Young S, Sy JS, et al. **Tumefactive lesions in retinal vasculopathy with cerebral leukoencephalopathy and systemic manifestations (RVCL-S): a role for neuroinflammation?** *J Neurol Neurosurg Psychiatry* 2018;89:434–35 [CrossRef](#)
12. Carra-Dalliere C, Ayrignac X, Prieto-Morin C, et al. **TREX1 mutation in leukodystrophy with calcifications and persistent gadolinium-enhancement.** *Eur Neurol* 2017;77:113–14 [CrossRef Medline](#)
13. Gutmann DH, Fischbeck KH, Sergott RC. **Hereditary retinal vasculopathy with cerebral white matter lesions.** *Am J Med Genet* 1989;34:217–20 [CrossRef Medline](#)
14. Grand MG, Kaine J, Fulling K, et al. **Cerebroretinal vasculopathy: a new hereditary syndrome.** *Ophthalmology* 1988;95:649–59 [CrossRef Medline](#)
15. Raynowska J, Miskin DP, Pramanik B, et al. **Retinal vasculopathy with cerebral leukoencephalopathy (RVCL): a rare mimic of tumefactive MS.** *Neurology* 2018;91:e1423–28 [CrossRef Medline](#)
16. Hedderich DM, Lummel N, Deschauer M, et al. **Magnetic resonance imaging characteristics of retinal vasculopathy with cerebral leukoencephalopathy and systemic manifestations.** *Clin Neuroradiol* 2020;30:229–36 [CrossRef Medline](#)
17. Ford AL, Chin VW, Fellah S, et al. **Lesion evolution and neurodegeneration in RVCL-S: a monogenic microvasculopathy.** *Neurology* 2020;95:e1918–31 [CrossRef Medline](#)
18. Saito R, Nozaki H, Kato T, et al. **Retinal vasculopathy with cerebral leukodystrophy: clinicopathologic features of an autopsied patient with a heterozygous TREX 1 mutation.** *J Neuropathol Exp Neurol* 2019;78:181–86 [CrossRef](#)